Supporting Information

Quantum Spin Sensor for Open-shell Molecules

Shahjad Ali and Md. Ehesan Ali*

Institute of Nano Science and Technology, Sector-81, Mohali, Punjab-140306, India

E-mail: ehesan.ali@inst.ac.in

Contents

S1 Electronic structure of molecules adsorbed 4ZGNRH

The closed-shell N_2, CO and CO_2 are physisorbed on 4ZGNRH independent of the adsorption site. The optimized geometries of CO and CO_2 adsorbed 4ZGNRH in different configurations is shown in Figure S1. The perpendicular distance (d_m) between the adsorbed closed-shell molecule and 4ZGNRH is in the range 2.73-2.82Å. While open-shell O_2, NO and NO_2 are chemisorbed at the edges and physisorbed at the middle of 4ZGNRH. The chemisorption it is 2.15Å and 2.14Å for the upper and lower edges of 4ZGNRH respectively. The bond length $C_{z3} - O1$ and $C_{z4} - O1$ is 2.261Å and 2.309Å when $O2$ is chemisorbed at lower edge. The perpendicular distance between NO and 4ZGNRH is 2.46Å when physisorbed at the middle of 4ZGNRH. The bond length, $C_{z4} - N$, is 1.694Å when NO is chemisorbed at the lower edge of 4ZGNRH. Similarly, $C_{z4} - N$ is 1.636Å when NO_2 is chemisorbed at the lower edge of 4ZGNRH.

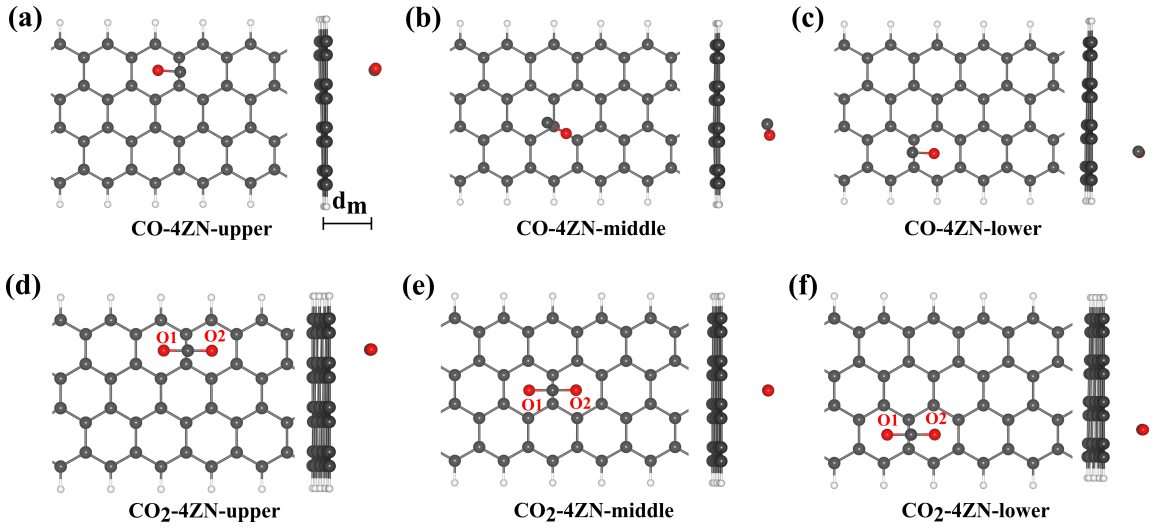

Figure S1: (a-f) The optimized structure of CO and CO_2 adsorbed 4ZGNRH in different configurations. The carbon, oxygen, and hydrogen atoms are represented by black, red, and gray balls, respectively.

Table S1: The bond lengths (in Å) of isolated molecules and after adsorption on 4ZGNRH in different configurations.

	Bond	Bond length (Å)		Bond	Bond length (Å)
isolated N_2	$N1-N2$	1.115	isolated O_2	$O1-O2$	1.237
N_2-4ZN-*upper*	$N1-N2$	1.117	O_2-4ZN-*upper*	$O1-O2$	1.263
N_2-4ZN-*middle*	$N1-N2$	1.117	O_2-4ZN-*middle*	$O1-O2$	1.244
N_2-4ZN-*lower*	$N1-N2$	1.117	O_2-4ZN-*lower*	$O1-O2$	1.260
isolated CO	$C-O$	1.146	isolated NO	$N-O$	1.257
CO-4ZN-*upper*	$C-O$	1.147	NO-4ZN-*upper*	$N-O$	1.287
CO-4ZN-*middle*	$C-O$	1.147	NO-4ZN-*middle*	$N-O$	1.265
CO-4ZN-*lower*	$C-O$	1.147	NO-4ZN-*lower*	$N-O$	1.287
isolated CO_2	$C-O1$	1.179	isolated NO_2	$N-O1$	1.296
	$C-O2$	1.179		$N-O2$	1.296
CO_2-4ZN-*upper*	$C-O1$	1.178	NO_2-4ZN-upper	$N-O1$	1.270
	$C-O2$	1.178		$N-O2$	1.558
CO_2-4ZN-*middle*	$C-O1$	1.178	NO_2-4ZN-middle	$N-O1$	1.310
	$C-O2$	1.178		$N-O2$	1.309
CO_2-4ZN-*lower*	$C-O1$	1.178	NO_2-4ZN-lower	$N-O1$	1.303
	$C-O2$	1.179		$N-O2$	1.303

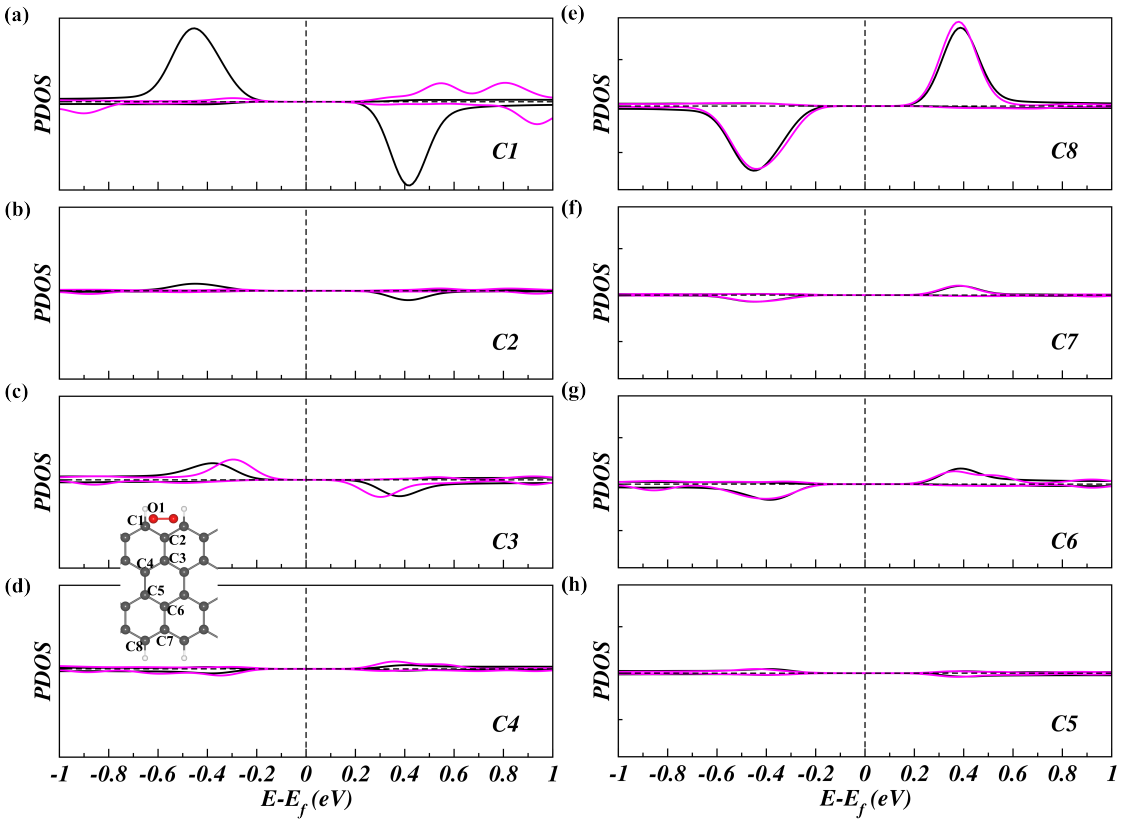

Figure S2: Atom-resolved partial density of states of carbon atoms of pristine 4ZGNRH and O_2-4ZN-upper. The PDOS of pristine 4ZGNRH and O_2-4ZN-upper are shown with black and magenta colors respectively.

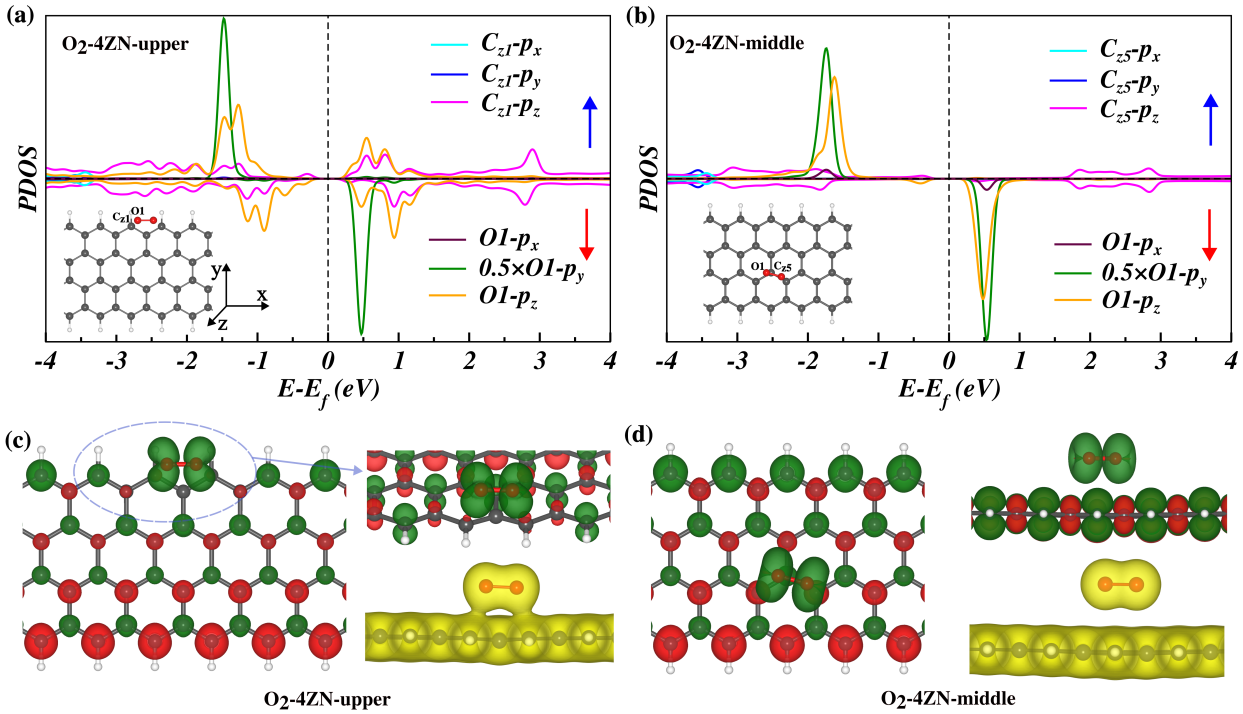

Figure S3: Orbital-resolved projected density of states (PDOS) of (a) C_{z1} carbon atom of 4ZGNRH and $O1$ oxygen atom of O_2 in O_2-4ZN-upper configuration and (b) C_{z5} carbon atom of 4ZGNRH and $O1$ oxygen atom of O_2 in O_2-4ZN-middle configuration. The spin-up (spin-down) PDOS are marked with blue and red arrows. The Fermi level is represented by a vertical dotted line. (c, d) spin and total charge density plots of O_2-4ZN-upper and O_2-4ZN-middle configurations at the iso-surface value of 0.2 au. The spin-up (spin-down) density of states are shown with green (red) color. The total charge density is shown in yellow color.

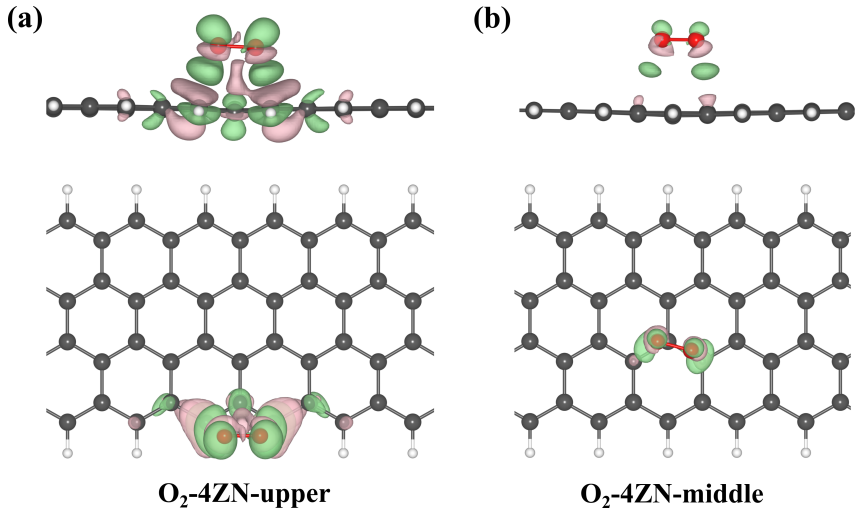

Figure S4: (a, b) Charge density difference of O_2-4ZN-upper and O_2-4ZN-middle configurations. The accumulation and depletion of charge density are shown with green and purple colors respectively. Charge density difference are plotted at the iso-surface value of 0.01 au.

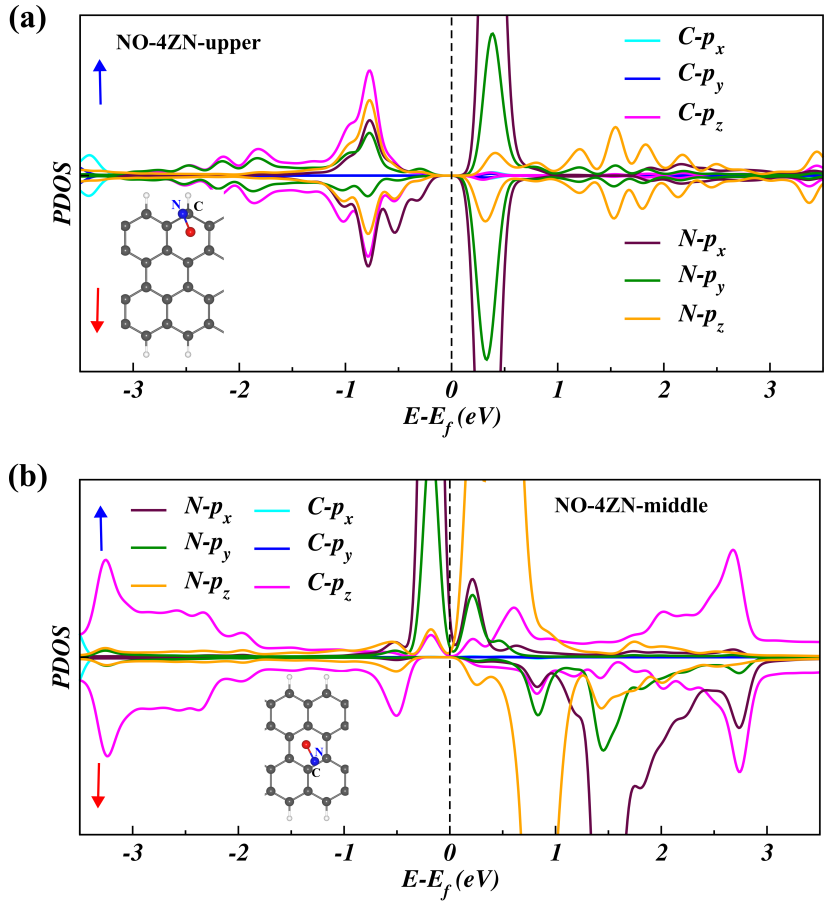

Figure S5: (a, b) Orbital-resolved partial density of states of carbon atom of 4ZGNRH and nitrogen atom of NO in NO-4ZN-upper and NO-4ZN-middle configuration.

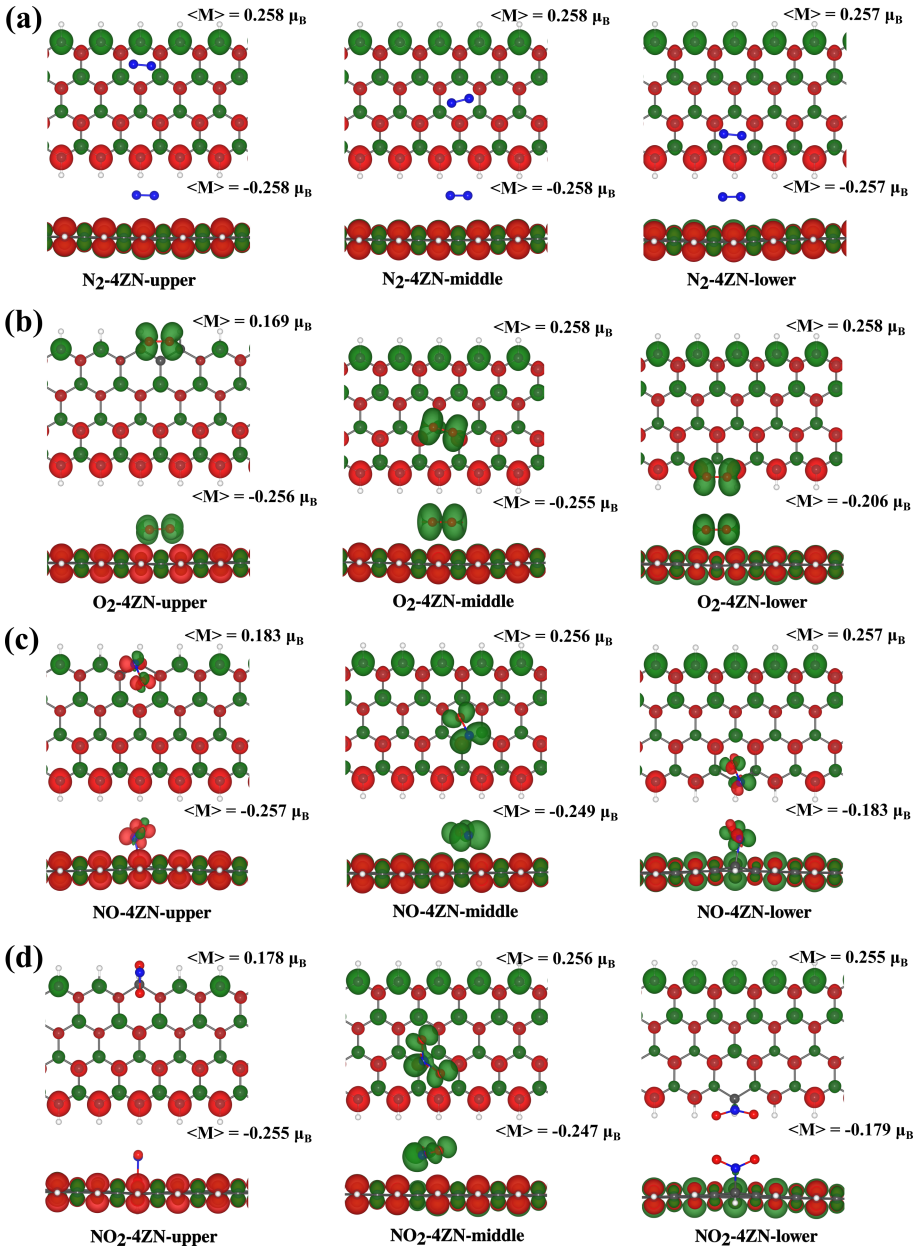

Figure S6: (a-d) The spin density plots of N_2, O_2, NO and NO_2 adsorbed 4ZGNRH in different geometric configurations. The spin-up (spin-down) density is shown with a green (red) color at an isosurface value of $0.02\mu_B$Å^{-3}. $< M >$ represents the average magnetic moment of the edge carbon atoms of 4ZGNRH.

S2 Electron transmission in pristine ZGNRs

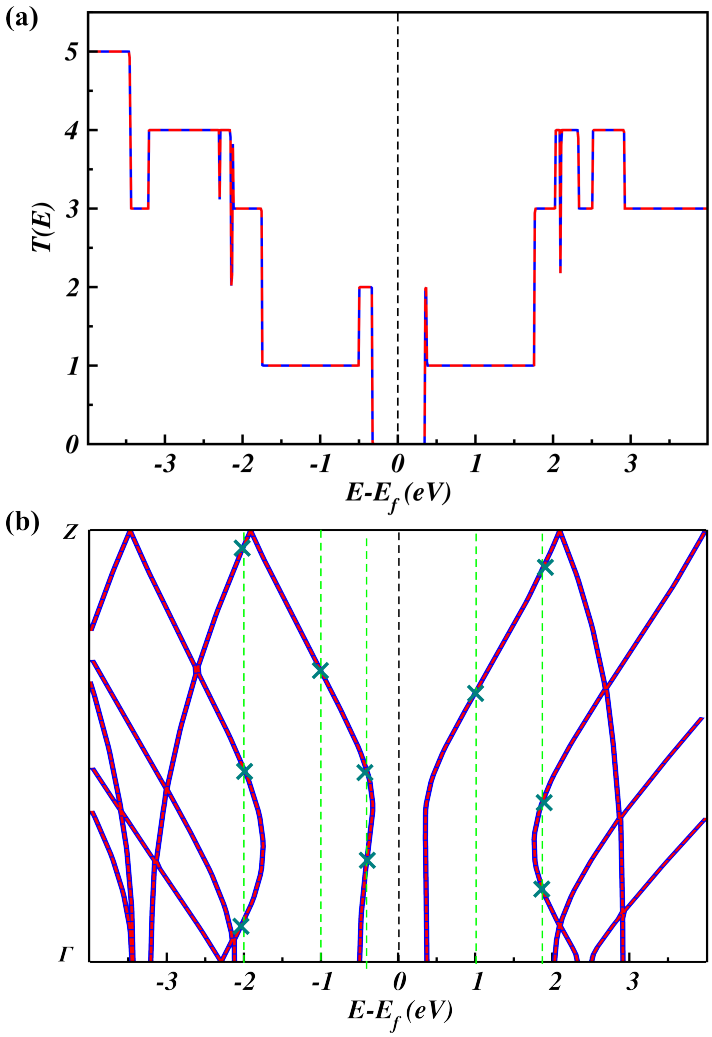

Figure S7: (a) Spin-resolved transmission spectra and (b) band structure of pristine 4ZGNRH. The spin-up (spin-down) transmission spectra and band structure are shown with blue (red) curves.

Transmission spectra of pristine 4ZGNRH show a transmission gap of 0.72 eV at the Fermi level, which corresponds to the band gap of 4ZGNRH (0.72 eV). Apart from that, 4ZGNRH shows plateau-like conductance features and spin-degenerate transmission spectra. The plateau-like conductance feature originates from the multi-channel ballistic transport of electrons. The conductance changes in integral steps depending on the number of transmission

channels, which is proportional to the number of occupied transverse sub-bands as shown in Figure S7.

S3 Electron transmission in closed-shell molecule adsorbed 4ZGNRH

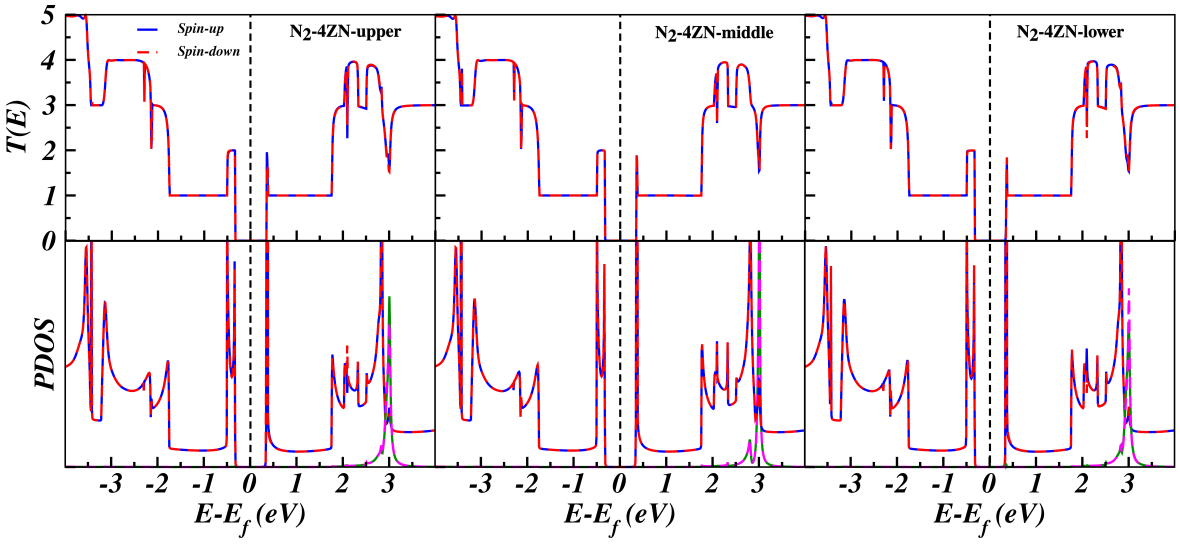

Figure S8: The spin-polarized electron transmission spectra of N_2 adsorbed 4ZGNRH in different geometric configurations. The spin-up (spin-down) transmission spectrum and PDOS of 4ZGNRH are shown with a blue (red) color. The spin-up (spin-down) PDOS of adsorbed molecules is shown with a green (magenta) color. The Fermi energy level is denoted with a vertical black dotted line.

The calculated transmission spectra and partial density of states of CO and CO_2 adsorbed 4ZGNRH are shown in Figure S9 and Figure S10. The adsorption of closed-shell CO and CO_2 molecules does not result in any significant changes in the transmission spectra of pristine 4ZGNRH near the Fermi level. The adsorption of CO shows a transmission dip near $E-E_f = -3.86eV$ and $E-E_f = 3.0eV$ for both spin-up and spin-down transmission spectra. Similarly, the adsorption of CO_2 shows a transmission dip near $E-E_f = -4.27eV$ and $E-E_f = 4.3eV$ for both spin-up and spin-down transmission spectra. Partial density of states (PDOS) of the adsorbed CO and CO_2 molecules and 4ZGNRH shows that PDOS of adsorbed

molecules corresponds to the position of the transmission dips in the transmission spectra of the molecule adsorbed 4ZGNRH. Thus, destructive interference between the molecular states and the continuum states of the 4ZGNRH results in such transmission dips.

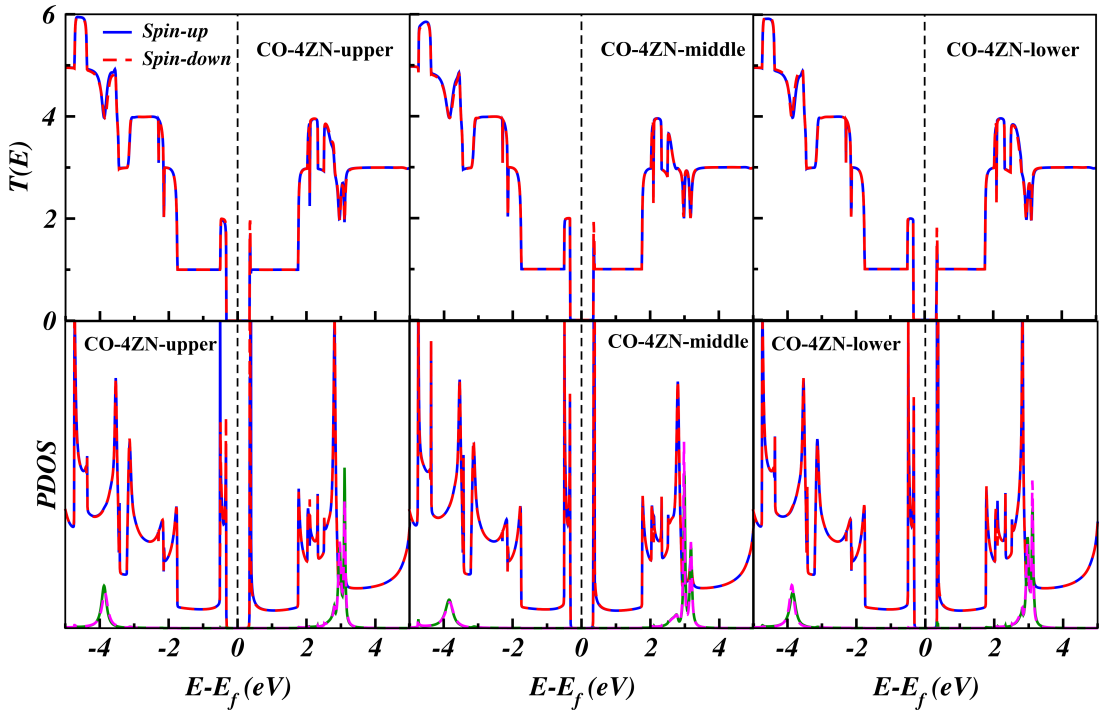

Figure S9: The spin-polarized electron transmission spectra and partial density of states of *CO* adsorbed 4ZGNRH in different geometric configurations. The spin-up (spin-down) transmission spectrum and PDOS of 4ZGNRH are shown with a blue (red) color. The spin-up (spin-down) PDOS of adsorbed molecules is shown with a green (magenta) color. The Fermi energy level is denoted with a vertical black dotted line.

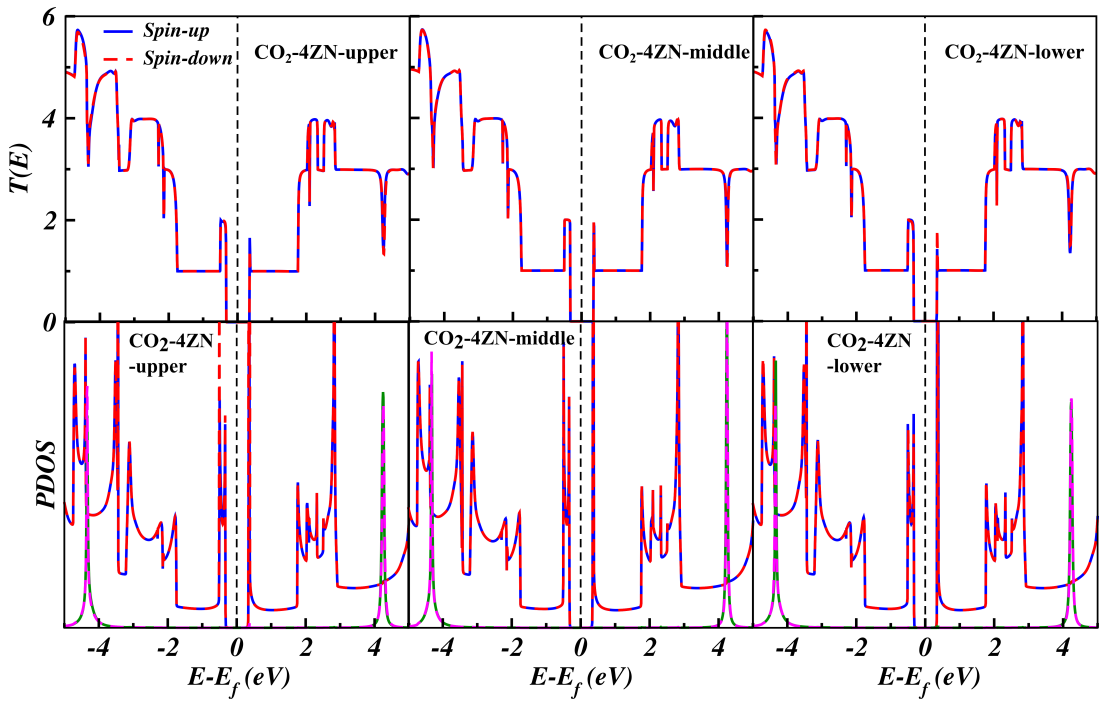

Figure S10: The spin-polarized electron transmission spectra and partial density of states of CO_2 adsorbed 4ZGNRH in different geometric configurations. The spin-up (spin-down) transmission spectrum and PDOS of 4ZGNRH are shown with a blue (red) color. The spin-up (spin-down) PDOS of adsorbed molecules is shown with a green (magenta) color. The Fermi energy level is denoted with a vertical black dotted line.

S4 Electron transmission in open-shell molecule adsorbed 4ZGNRH

The adsorption of O_2 molecule on the upper edge of 4ZGNRH results in the localized spin-up (spin-down) states at energy -0.275 eV (0.295 eV). The density of states analysis of the upper edge carbon atoms of device region for O_2-4ZN-*upper* configuration (shown in Figure S12). For convenience, we have numbered the edge carbon atoms of device region from C1 to C9 as shown in Figure S12(b). The O_2 atom is chemisorbed at C5 and C6. The atom-resolved PDOS analysis shows that the spin-up (spin-down) state at energy -0.275 eV (0.295 eV) are contributed mainly from C1 to C4 and C7 to C9 edge carbon atoms. It has comparatively very small contribution from the C5 and C6 edge carbon atoms and O_2 molecule. Thus, the

adsorption of O_2 molecule at the upper edge of the 4ZGNRH, breaks the π conjugation of the upper edge carbon atoms. It lower the energy of the spin-up highest occupied energy level from -0.345 eV to -0.275 eV (see Figure S11 and Figure S12). These edge localized states result in resonant transmission peaks instead of the destructive quantum interference (DQI) due to absence of states in the electrodes which have a band gap 0.72 eV (pristine 4ZGNRH).

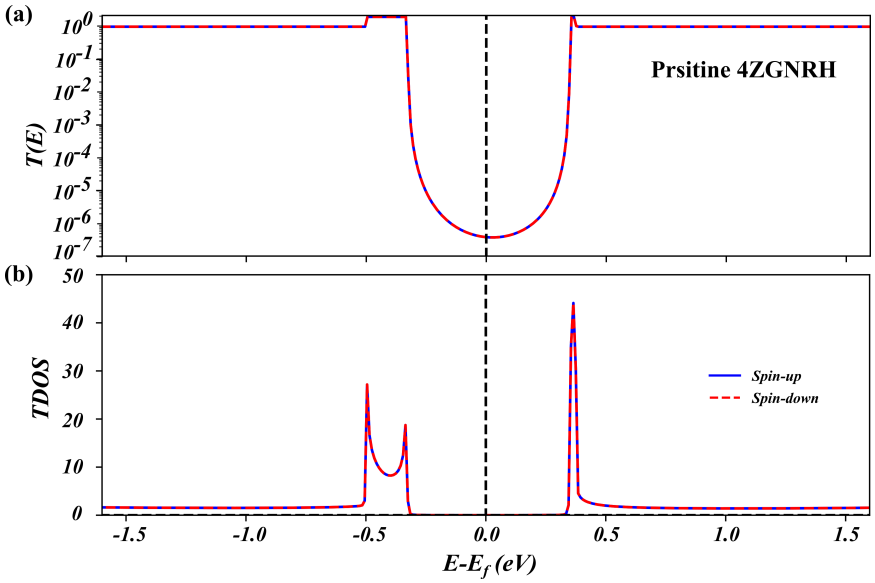

Figure S11: (a, b) The spin-polarized electron transmission spectra and total density of states (TDOS) of the pristine 4ZGNRH. The spin-up (spin-down) transmission spectrum and TDOS are shown in blue (red). The Fermi energy level is denoted with a vertical black dotted line.

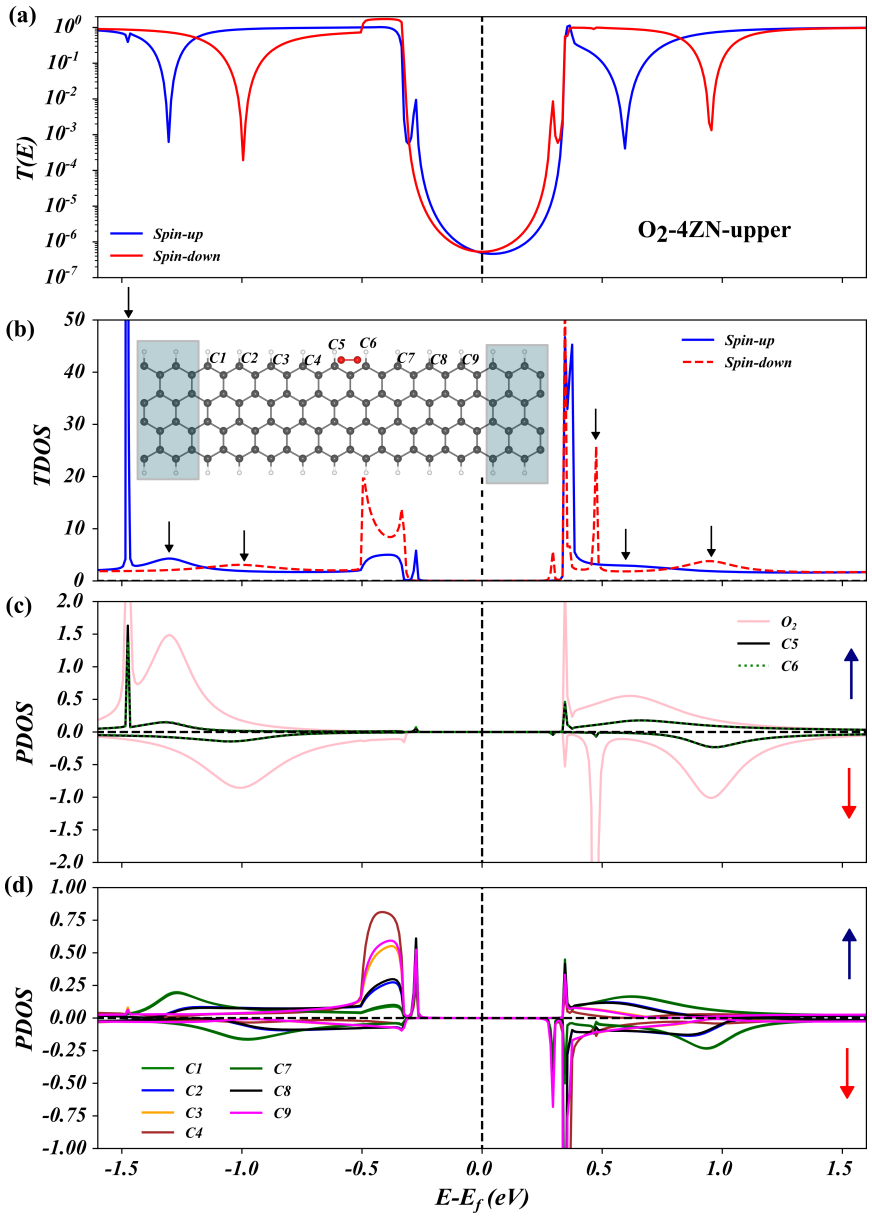

Figure S12: (a, b) The spin-polarized electron transmission spectra and total density of states (TDOS) of O_2 adsorbed 4ZGNRH at upper edge of ZGNR. The spin-up (spin-down) transmission spectrum and TDOS are shown in blue (red). (c, d) Partial density of states (PDOS) of oxygen molecule and upper edge carbon atoms. The spin-up (spin-down) PDOS are shown on positive (negative) y-axis. The Fermi energy level is denoted with a vertical black dotted line.

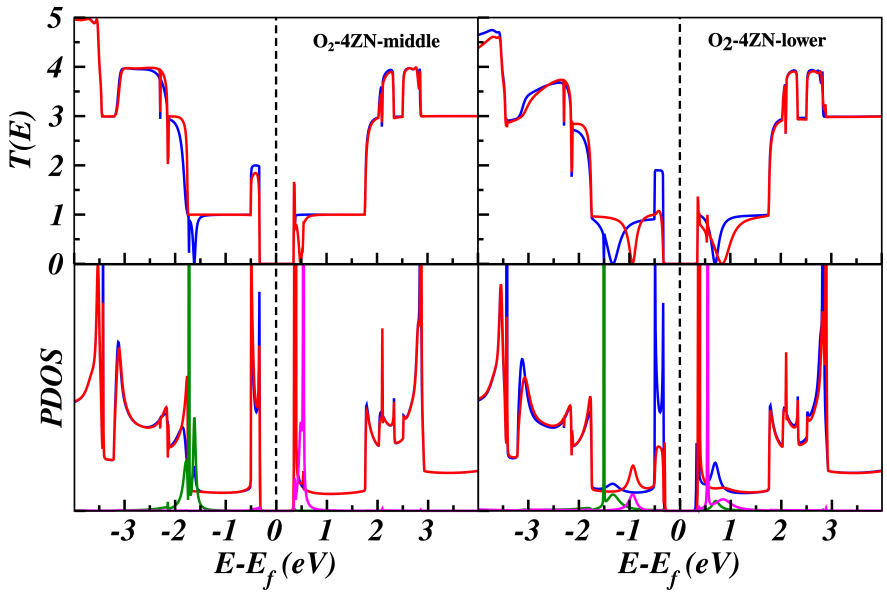

Figure S13: The spin-polarized electron transmission spectra and partial density of states of O_2 adsorbed 4ZGNRH in different geometric configurations. The spin-up (spin-down) transmission spectrum and PDOS of 4ZGNRH are shown with a blue (red) color. The spin-up (spin-down) PDOS of adsorbed molecules is shown with a green (magenta) color. The Fermi energy level is denoted with a vertical black dotted line.

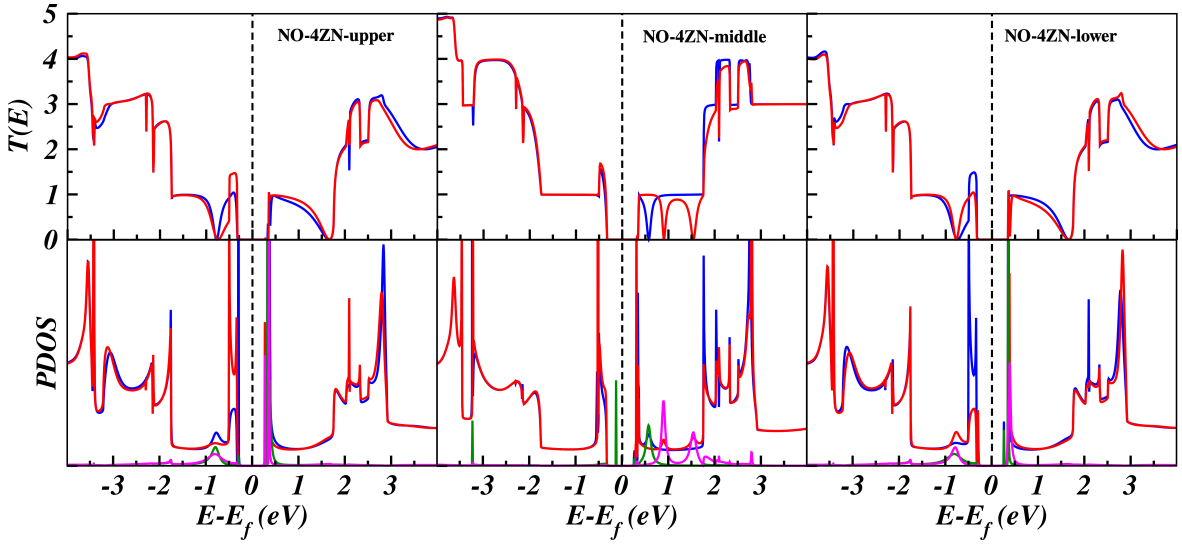

Figure S14: The spin-polarized electron transmission spectra and partial density of states of NO adsorbed 4ZGNRH in different geometric configurations. The spin-up (spin-down) transmission spectrum and PDOS of 4ZGNRH are shown with a blue (red) color. The spin-up (spin-down) PDOS of adsorbed molecules is shown with a green (magenta) color. The Fermi energy level is denoted with a vertical black dotted line.

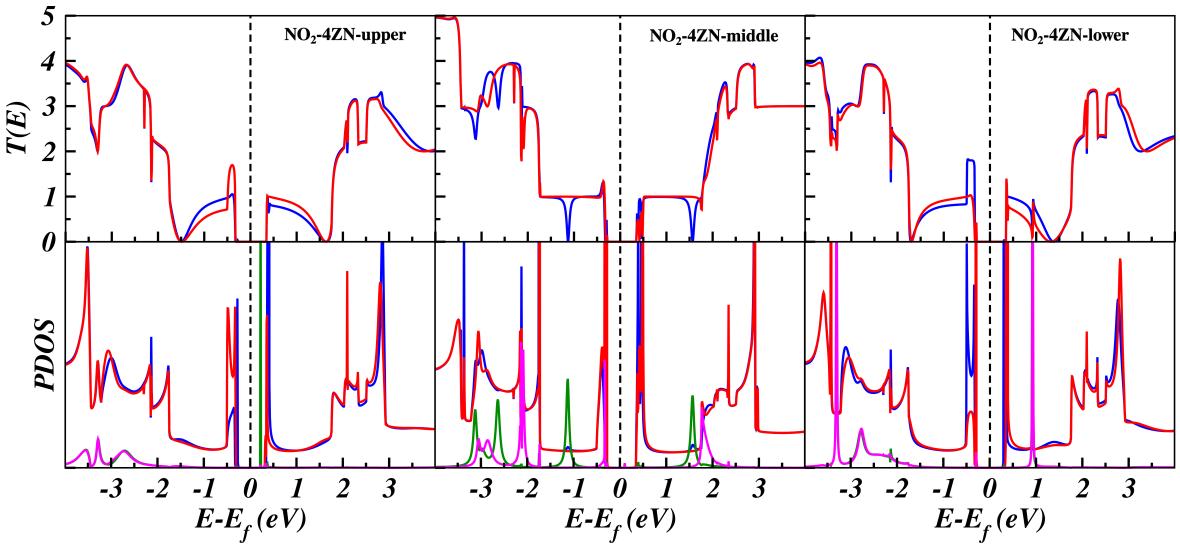

Figure S15: The spin-polarized electron transmission spectra and partial density of states of NO_2 adsorbed 4ZGNRH in different geometric configurations. The spin-up (spin-down) transmission spectrum and PDOS of 4ZGNRH are shown with a blue (red) color. The spin-up (spin-down) PDOS of adsorbed molecules is shown with a green (magenta) color. The Fermi energy level is denoted with a vertical black dotted line.

S5 Effects of bias voltage

The current versus bias voltage characteristics of CO and CO_2 deposited 4ZGNRH are shown in figure S16(a-f). Current under the application of bias voltage (V_b) depends on the transmission spectra within the bias window $(-V_b/2,\ V_b/2)$ around the Fermi level. Adsorption of non-magnetic molecules results in a decrease in spin-up and spin-down current with respect to the pristine 4ZGNRH for $V_b < 1.7V$.

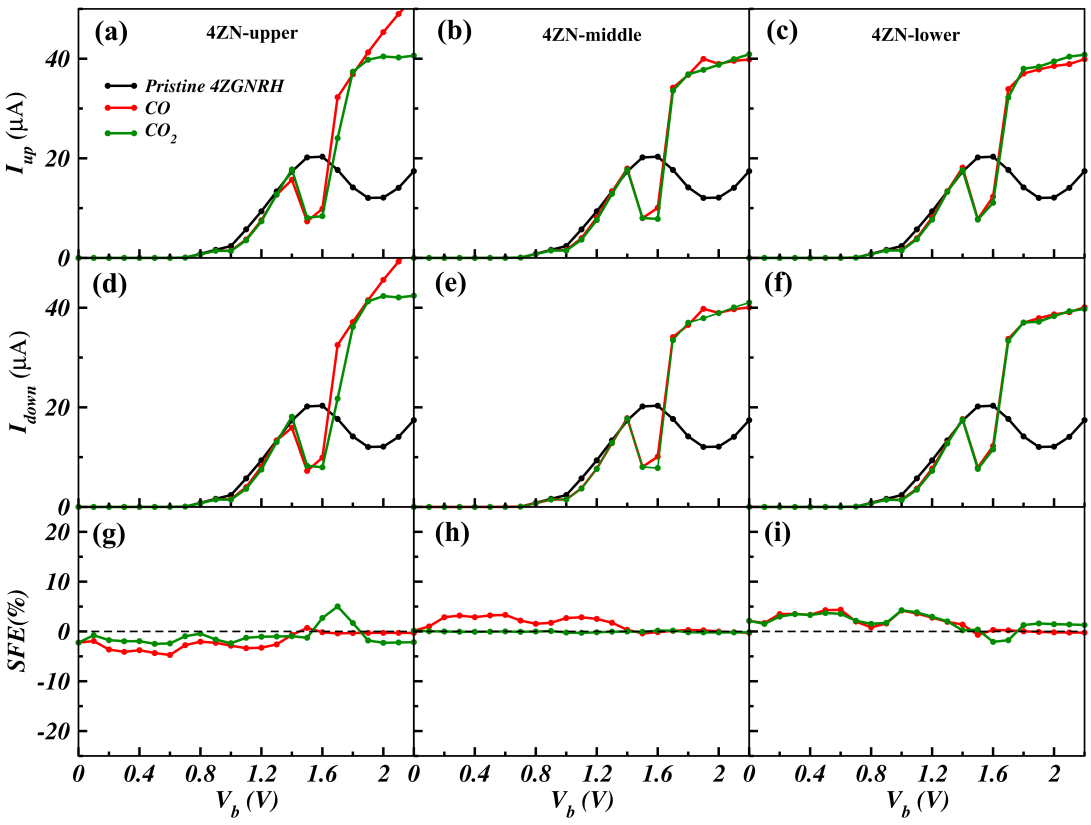

Figure S16: (a-f) Comparison of (a-c) spin-up (d-f) spin-down and (g-j) spin-filtering efficiency (SFE) of CO and CO_2 adsorbed in different configurations on 4ZGNRH.

S6 Inelastic Transport

To check the effect of molecular vibrations on the transport properties of molecule adsorbed ZGNRs, we have calculated the inelastic electron transport for O_2-4ZN-*upper* case. We have only considered the effect of vibrations of O_2 molecule. It has total six vibrational modes whose corresponding energy and corresponding displacement of O_2 atoms are shown in Figure S17 and Figure S18. Further, the spin polarized current comparison shows that unlike the elastic transport, inelastic transport results in increased spin-down current as compared to spin-up current (shown in Figure S19). The resulting SFE is -5.17% which is comparable to 4.68% SFE of elastic transport. However, it should should be noted that a full self-consistent field (SCF) approach is adopted for the bias voltage calculations for

elastic transport using Transiesta. While in case of inelastica transport calculations, a non-SCF approach has been utilized for the bias voltage calculations using the zero bias full SCF Tansiesta solutions. To check the effect of phonon on the conductance, we have computed the inelastic electron tunneling spectroscopy (IETS) as shown in Figure S20. The IETS is the ratio of the change in the differential conductance to the differential conductance.

$$IETS(1/V) = \frac{d^2I/d^2V}{dI/dV} \tag{1}$$

The IETS spectra shows that the molecular vibrations have small effect on the change in the differential conductance ($\sim$ 0.06 $1/V$). And this effect is negligibly small for the differential conductance. For example, there is 6.5×10^{-8} G_o (7.3×10^{-8} G_o) decrease in the spin-up (spin-down) differential conductance due to phonon mode at energy $\sim$ 0.05 (mode index 2) which $\sim$ 0.06% decrease. Thus, the molecular vibrations have quite small impact on the spin-dependent conductance and the it does not have any significant effect on the resulting spin filtering efficiency (SFE).

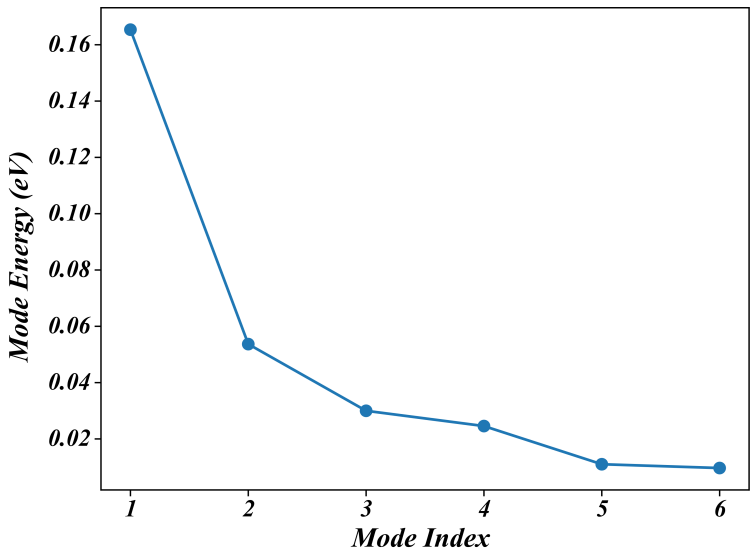

Figure S17: Vibrational frequencies calculated for O_2 in O_2-4ZN-*upper* configurations. All the atoms of 4ZGNRH were fixed.

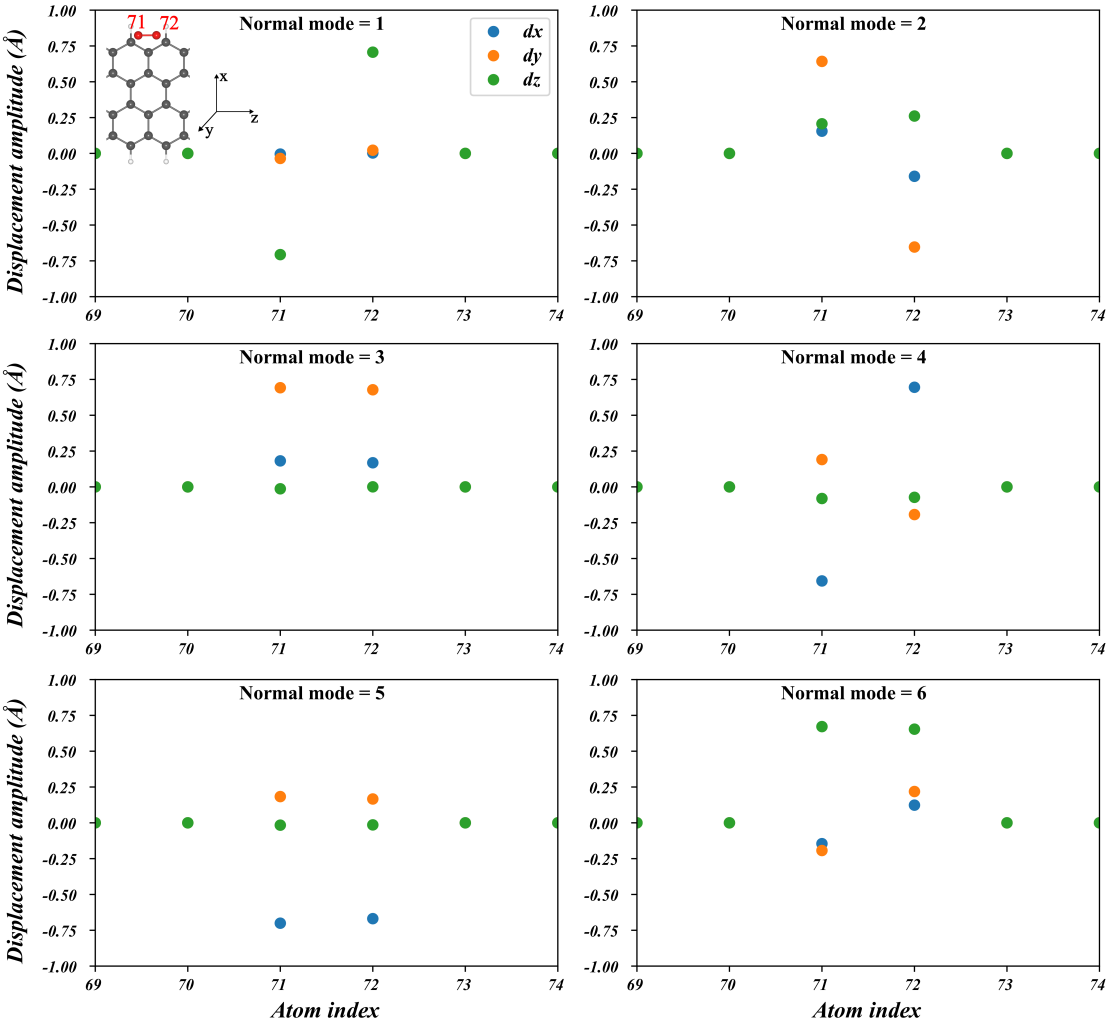

Figure S18: The atomic displacement of O_2-4ZN-*upper* atoms for the different vibrational modes.

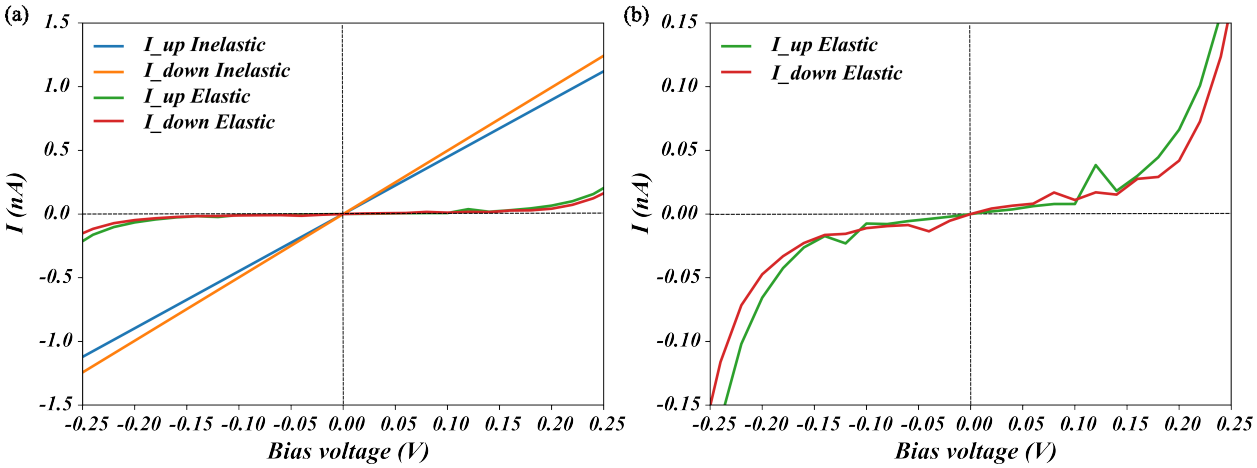

Figure S19: (a, b) Comparison of elastic and inelastic spin current. The elastic current is calculated using the Transiesta method while inelastic current is calculated using the Inelastica package.

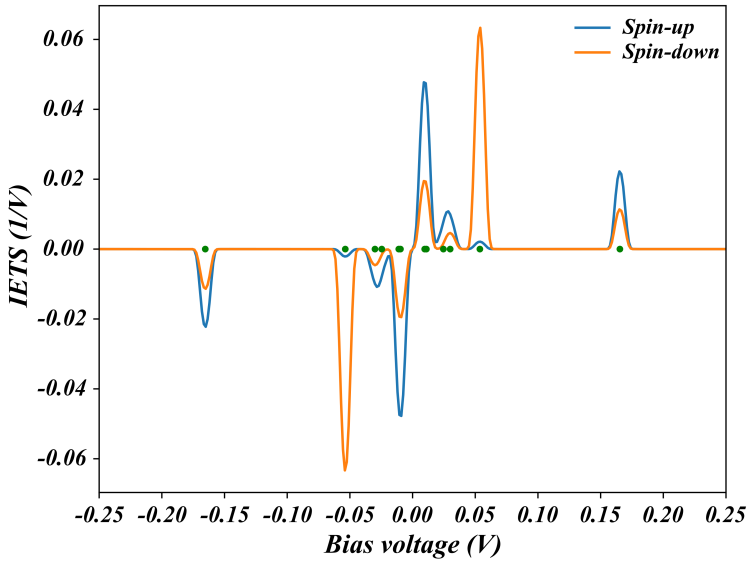

Figure S20: Calculated IETS spectrum for O_2-4ZN-*upper*. Each of the inelastic scattering peaks arise from different kinds of vibrations localized on the O_2 molecule.